JOURNAL OF VIROLOGY, Jan. 2010, p. 109–118 Vol. 84, No. 1
0022-538X/10/$12.00 doi:10.1128/JVI.01428-09

Conserved Residues in the UL24 Protein of Herpes Simplex Virus 1 Are Important for Dispersal of the Nucleolar Protein Nucleolin▽

Luc Bertrand, Gabriel André Leiva-Torres,† Huda Hyjazie, and Angela Pearson*

INRS-Institut Armand-Frappier, Université du Québec, Laval, Québec, Canada

Received 10 July 2009/Accepted 20 October 2009

The UL24 family of proteins is widely conserved among herpesviruses. We demonstrated previously that UL24 of herpes simplex virus 1 (HSV-1) is important for the dispersal of nucleolin from nucleolar foci throughout the nuclei of infected cells. Furthermore, the N-terminal portion of UL24 localizes to nuclei and can disperse nucleolin in the absence of any other viral proteins. In this study, we tested the hypothesis that highly conserved residues in UL24 are important for the ability of the protein to modify the nuclear distribution of nucleolin. We constructed a panel of substitution mutations in UL24 and tested their effects on nucleolin staining patterns. We found that modified UL24 proteins exhibited a range of subcellular distributions. Mutations associated with a wild-type localization pattern for UL24 correlated with high levels of nucleolin dispersal. Interestingly, mutations targeting two regions, namely, within the first homology domain and overlapping or near the previously identified PD-(D/E)XK endonuclease motif, caused the most altered UL24 localization pattern and the most drastic reduction in its ability to disperse nucleolin. Viral mutants corresponding to the substitutions G121A and E99A/K101A both exhibited a syncytial plaque phenotype at 39°C. vUL24-E99A/K101A replicated to lower titers than did vUL24-G121A or KOS. Furthermore, the E99A/K101A mutation caused the greatest impairment of HSV-1-induced dispersal of nucleolin. Our results identified residues in UL24 that are critical for the ability of UL24 to alter nucleoli and further support the notion that the endonuclease motif is important for the function of UL24 during infection.

The UL24 protein is conserved throughout the *Herpesviridae* family, and to the best of our knowledge, a *UL24* homolog has been identified in all *Herpesvirales* genomes sequenced to date with the exception of the channel catfish virus (9, 10, 19). UL24 of herpes simplex virus 1 (HSV-1) is required for efficient virus replication both in vitro and in vivo and for reactivation from latency in a mouse model of ocular infection (18). *UL24* is one of the few HSV-1 genes, along with *gB*, *gK*, and *UL20*, in which mutations have been identified that cause the formation of syncytial plaques (2, 7, 34, 36, 39). The *UL24*-associated syncytial phenotype is only partially penetrant at 37°C but is fully penetrant at 39°C. Indications are that gK and UL20 have an inhibitory effect on the formation of syncytia (1), while certain mutations in gB entrain an uncontrolled fusogenic activity (11, 13, 15).

UL24 is a highly basic protein of 269 amino acids that is expressed with leaky-late kinetics (31). Five homology domains (HDs), which consist of stretches of amino acids with a high percentage of identity between homologs, are present in the *UL24* open reading frame (ORF) (19). In addition, a PD-(D/E)XK endonuclease motif has been identified that falls within the HDs (20); however, a role for this motif has yet to be demonstrated. In infected cells, UL24 is detected in the nucleus and the cytoplasm and transiently localizes to nucleoli (23). In the absence of other viral proteins, UL24 accumulates in the Golgi apparatus and in the nucleus, where it usually exhibits a diffuse staining pattern, but in a minority of cells it is detected in nucleoli (3).

During infection, the formation of the viral replication compartments in the nucleus and the action of several viral proteins result in a remodeling of the nucleus. Chromatin is marginalized (29, 40), promyelocytic leukemia bodies are dispersed (26, 27), and the nuclear lamina is disrupted (33, 37). HSV-1 infection also affects the nucleolus, a prominent nuclear substructure implicated in the synthesis of rRNA, cell cycle regulation, and nucleocytoplasmic shuttling (5). Nucleoli become elongated following infection, and the synthesis of mature rRNA is reduced (4, 38, 42). Several HSV-1 proteins have been shown to localize to, or associate with, the nucleolus (12). The viral protein VP22 associates with the nucleolus and with dispersed nucleolin in HSV-1-infected cells (22), and RL1, US11, and ICP0 have also been shown to localize to nucleoli (24, 30, 35). Previously we showed that nucleolin is dispersed throughout the nucleus upon HSV-1 infection and that UL24 is involved in this nuclear modification (23). We further found that the N-terminal portion of UL24 is sufficient to induce the redistribution of nucleolin in the absence of other viral proteins (3).

In this study, we sought to test the hypothesis that the endonuclease motif, which is made up of some of the most highly conserved residues in UL24, is important for the dispersal of nucleolin. A panel of substitution mutations in UL24 was generated, and the impact on the function of UL24 was assessed.

MATERIALS AND METHODS

Cells and viruses. Vero and COS-7 cells were propagated as described previously (3). The virus strains KOS and UL24XG (18) were generously provided by Donald M. Coen (Harvard Medical School). For the plaque morphology assays, infected cells were incubated in Dulbecco's modified Eagle medium containing

* Corresponding author. Mailing address: INRS-Institut Armand-Frappier, 531 Boulevard des Prairies, Laval, Québec, Canada. Phone: (450) 687-5010. Fax: (450) 686-5501. E-mail: angela.pearson@iaf.inrs.ca.

† Present address: McGill University, Department of Microbiology and Immunology, Montreal, Quebec, Canada.

▽ Published ahead of print on 28 October 2009.

high glucose with 0.33% methylcellulose and supplemented with 2% newborn calf serum, 50 U/ml of penicillin, and 50 μg/ml of streptomycin.

Plasmid construction. To generate mutations in the *UL24* gene, PCR site-directed mutagenesis was carried out on the plasmid pAG5 (16) or pLB-HA-UL24 (3). PCRs were performed using complementary sets of mutagenic oligonucleotides. DNA from the reactions was digested with DpnI (Roche) to remove the wild-type template DNA and ligated with T4 DNA ligase (New England Biolabs). Following transformation into DH5α bacteria, plasmids were sequenced to verify the presence of the desired mutation and the absence of other sequence changes in the *UL24* ORF. DNA sequencing was carried out by the McGill University and Genome Innovation Center. The different mutations and the corresponding mutagenic oligonucleotides used are as follows (nucleotide changes are represented by bold characters): for E69A/V70A, UL24E69AV70Atop (5′-GTCACCTTAATATGCG**C**AG**C**GGACCTGGGAC GGCGC) and UL24E69V70AAbot (5′-GCGCGGTCCCAGGTCC**G**CT**G**CGC ATATTAAGGTGAC); for L72A, UL24L72Atop (5′-GCGAAGTGGAC**GC**G GGACCGCGCCG) and UL24L72Abot (5′-CGGCGCGGTCCC**GC**GTCCACT TCGC); for R75A/D78A, UL24R75AD78Atop (5′-CCTGGGACC**GGC**CCGC CCCG**C**CTGCATCTGC) and UL24R75AD78Abot (5′-GCAGATGCAG**G**CG GGGCGG**GC**CGGTCCCAGG); for I97A/I98A, UL24I97AI98Atop (5′-CTGGGCGGGGTTTGTGTC**GC**C**GC**AGAACTAAAGACATGC) and UL24 I97AI98Abot (5′-GCATGTCTTTAGTTCT**GC**G**GC**GACACAAACCCCGCC CAG); for E99A/K101A, UL24E99K101Atop (5′-GGGTTTGTGTCATCATAG **C**ACTA**GC**GACATGCAAATATATTTCTTCCG) and UL24E99AK101Abot (5′-CGGAAGAAATATATTTGCATGTC**GC**TAGT**G**CTATGATGACACAA ACCC); for Q117A, UL24Q117Atop (5′-CGCCAGCAAACGCGAG**GC**ACGG GCCACGGGGATG) and UL24Q117Abot (5′-CATCCCCGTGGCCCGT**GC**C TCGCGTTTGCTGGCG); for G121A, UL24G121Atop (5′-GAGCAACGGGC CACGG**C**GATGAAGCAGCTGCGC) and UL24G121Abot (5′-GCGCAGC TGCTTCATCGCC**G**TGGCCCGTTGCTC); for Q124A/L125A, UL24 Q124/L125Atop (5′-GGGCCACGGGGATGAAG**GC**G**GC**GCGCCACTCCC TGAAGC) and UL24Q124A/L125Abot (5′-GCTTCAGGGAGTGGCGC**GC**C **GC**CTTCATCCCCGTGGCCC); for Q154A, UL24Q154Atop (5′-CCTGGTGT TTGTCGCC**GC**ACGGACGCTCCGCGTC) and UL24Q154Abot (5′-GA CGCGGAGCGTCCGT**GC**GGCGACAAACACCAGG); for H22L, UL24 H22Ltop (5′-GCAGGGGTACGAAGCC**T**TACGCGCTTCTACAAG) and UL24H22Lbot (5′-CTTGTAGAAGCGCGTAA**G**GCTTCGTACCCCTGC); and for Y26A, UL24Y26Atop (5′-CGAAGCCATACGCGCTTC**GC**CAAGGC GCTTGCCAAAG) and UL24Y26Abot (5′-CTTTGGCAAGCGCCTTG**GC**GA AGCGCGTATGGCTTCG).

For all mutations other than H22L and Y26A, mutagenesis was performed on the plasmid pAG5, and the mutations were then subcloned into the mammalian expression vector pLBPfl-HA-UL24. For the substitutions H22L and Y26A, mutagenesis was performed on the plasmid pLB-HA-UL24, which was then subcloned back into pLBPfl-HA-UL24 in case mutations had arisen in the rest of the vector during the mutagenesis step.

The plasmid pBamHIQeGFP was obtained by the insertion of an expression cassette containing the cytomegalovirus (CMV) promoter driving the enhanced green fluorescent protein (eGFP) gene into the Bsp119I site of pAG5. The CMV-eGFP cassette was amplified from the template pEGFP-N1 (Clontech) using the primers eGFP-CMVp-Start (5′-TTCGAATAGTTATTAATAGTAA TCAATTACG-3′) and eGFP-STOP-End (5′-TTCGAAATCTAGAGTCGCGG CCGC-3′), which contain Bsp119I sites at their 5′ ends. The PCR fragment was inserted in the pCR-BluntII-TOPO vector (Invitrogen) and then digested with Bsp119I (New England Biolabs) along with the vector pAG5; these were ligated together using T4 DNA ligase.

Transfection and Western blotting. To assess expression of hemagglutinin epitope (HA)-tagged UL24 proteins, 1.5×10^5 COS-7 cells were seeded per well in six-well plates. The following day, cells were transfected with 3 μg of pLBPfl-HA-UL24 or a mutant version using the Lipofectamine transfection reagent (Invitrogen) according to the manufacturer's instructions. Two days posttransfection, cells were washed with phosphate-buffered saline (PBS) and lysed in 150 μl of RIPA lysis buffer (500 mM NaCl, 1% Triton X-100, 0.5% deoxycholic acid, 0.1% sodium dodecyl sulfate, and 50 mM Tris [pH 8.0]). A 0.2-μg amount of a β-galactosidase expression vector was cotransfected to normalize loading according to transfection efficiency. β-Galactosidase activity was quantified using the luminescent β-galactosidase detection kit II (Clontech), following the manufacturer's instructions. Normalized volumes of lysate were resolved by polyacrylamide gel electrophoresis on a denaturing sodium dodecyl sulfate 12.5% gel. For infected cell lysates, Vero cells were infected at a multiplicity of infection (MOI) of 10 and lysed in RIPA lysis buffer at 18 h postinfection (hpi). Proteins were transferred to a polyvinylidene difluoride membrane (Immobilon-P; Millipore) and analyzed by Western blotting using a monoclonal antibody directed against HA (Covance) and a secondary antibody conjugated to horseradish peroxidase (Calbiochem). Detection was by enhanced chemiluminesence using ECL plus reagents (GE-Amersham).

Construction of recombinant viruses. Recombinant viruses were produced by homologous recombination essentially as described previously (16). The virus vUL24-eGFP was obtained by cotransfecting KOS infectious DNA and the transfer plasmid pBamHIQeGFP that had been linearized with XbaI (New England Biolabs). Recombinant viruses with mutant versions of *UL24* or, in the case of the rescue virus, wild-type *UL24* were obtained by cotransfection of vUL24-eGFPb infectious DNA and the appropriate linearized transfer vector: pAG5 for the rescue virus and pKOS-UL24-E99A/K101A or pKOS-UL24-G121A for the mutant viruses. DNA was transfected into Vero cells using Lipofectamine (Invitrogen) according to the manufacturer's instructions. Recombinant viruses engineered to express eGFP or to contain other forms of altered *UL24* genes were screened for the presence or absence of eGFP expression, respectively. The *UL24* ORF of each recombinant virus was sequenced to ensure the absence of undesired mutations.

Viral growth curves. Viral yield was assayed using one-step growth curves. Vero cells (2.5×10^5) were seeded in duplicate in cell culture tubes containing 2 ml of complete medium. The next day, cells were infected with the indicated virus at an MOI of 5. At 6, 12, 18, and 24 hpi, the respective tubes were removed from the incubator and placed at −80°C. Tubes were thawed and sonicated, and total virus (cell associated and cell free) was titrated.

Southern blotting. The overall genome structures of vUL24-eGFPb and -c and vUL24-eGFPResc were analyzed by restriction digest with BamHI. Viral genomic DNA was isolated by phenol-chloroform extraction of isolated virions. A 1.5-μg amount of viral DNA was digested with BamHI (New England Biolabs), as was 100 ng of the plasmid pAG5, which contains the wild-type BamHI Q fragment, and pBamH1QeGFP, which is the original transfer plasmid used for the construction of vUL24-eGFP. Restriction digest products were run on an agarose gel and transferred by capillarity action to a positively charged nylon membrane. The membrane was then blotted with a digoxigenin-labeled probe corresponding to the wild-type BamHI Q fragment in pBluescript II SK(+). The probe was generated using a random priming DNA labeling kit (Roche) according to the manufacturer's instructions. The signal was detected using the substrate disodium 3-(4-methoxyspiro{1,2-dioxetane-3,2′-(5′-chloro)tricyclo[3.3.1.13,7]decan}-4-yl)phenyl phosphate (Roche).

Immunofluorescence. Transient transfection of COS-7 cells was performed as described previously (3). For analysis of infected cells, 4×10^4 Vero cells were seeded on glass coverslips the day before infection at an MOI of 10 and fixed 18 hpi. Cells were immunostained as described previously (3). The following primary antibodies were used, as needed: rat monoclonal anti-HA high affinity (Roche), rabbit polyclonal anti-nucleolin (Abcam), and mouse monoclonal antinucleolin (Santa Cruz). Secondary antibodies used were goat anti-rat Alexa-488 conjugated and goat anti-mouse or anti-rabbit Alexa-568 conjugated (Invitrogen), as appropriate. After immunostaining, cells were washed three times in PBS and incubated with Draq5 (Biostatus) diluted 1:500 in PBS at 37°C for 30 min. The cells were then washed once in PBS, and coverslips were mounted on glass slides using the Prolong Gold antifade reagent (Invitrogen). The slides were visualized using a Bio-Rad Radiance 2000 confocal system with an argon-krypton laser at 488 and 568 nm (diode, 638 nm) mounted on a Nikon E800 microscope using a 60× objective, with an aperture of 1.4, and a 1.6× software magnification in the Lasersharp software program (Bio-Rad). Images were prepared using Adobe Photoshop CS4 software.

RESULTS

Replacement of highly conserved residues in UL24. The five UL24 HDs in HSV-1 UL24 contain clusters of amino acids that have a high degree of identity between UL24 proteins encoded by different herpesviruses. Previously we deleted each of these HDs individually and found that removal of any one resulted in a protein that localized efficiently to nucleoli but no longer caused the dispersal of nucleolin (3). We hypothesized that this lack of activity was a result of misfolding of the protein due to these relatively large deletions. Thus, in order to identify regions in UL24 that were important for its effect on nucleoli, we undertook a strategy of site-directed mutagenesis. We compared UL24 of HSV-1 (strain KOS) and several other UL24 homologs. Based on this analysis, we generated a panel

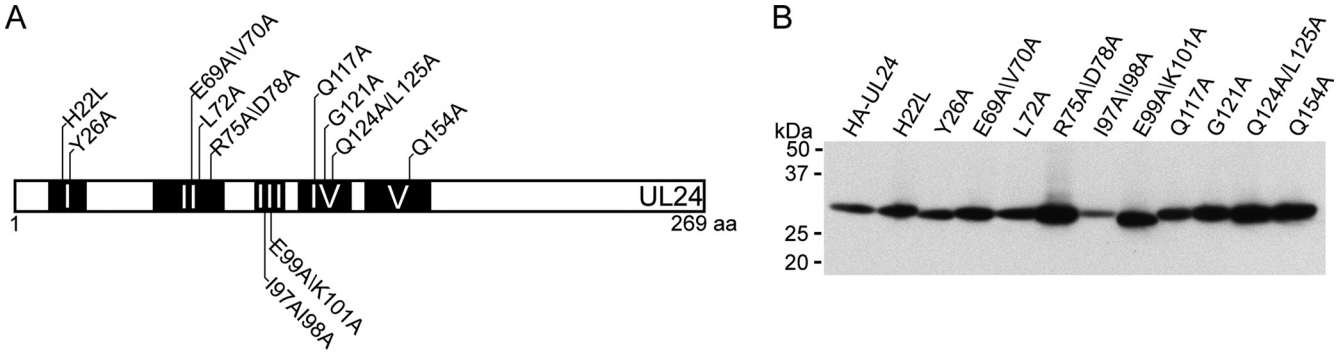

FIG. 1. Substitutions introduced into HSV-1 UL24. (A) The large rectangle represents the UL24 protein. Black boxes illustrate the positions of the five homology domains, numbered one to five in Roman numerals. The different single and double substitutions studied are indicated above or below the rectangle. (B) Expression of the different versions of HA-UL24 as detected by Western blot analysis of lysates prepared from transiently transfected COS-7 cells, using an antibody directed against the HA tag. Positions of molecular mass markers are indicated to the left of the panel.

of modified versions of UL24, where some of the most conserved residues were replaced individually or in pairs, namely, H22 (100% identity among 78 UL24 homologs), Y26 (99% identity), E69 (100%)/V70 (94%), L72 (96%), R75 (100%)/D78 (100%), I97 (58%)/I98 (68%), E99 (100%)/K101 (100%), Q117 (100%), G121A (100%), Q124A (99%)/L125A (97%), and Q154 (92%). The mutations generated are represented in Fig. 1A. The residues D78, E99, and K101 are part of the PD-(D/E)XK endonuclease motif. H22 and Y26, while not part of the motif, are residues that are conserved among several members of this family of endonucleases and have been proposed to play a role in substrate specificity (14, 20, 21). Mutations in the HA-*UL24* gene were introduced into the mammalian expression vector pLBPfl-HA-UL24. To assess protein expression, the vectors encoding different versions of HA-UL24, either wild-type or with point mutations, were transiently transfected into COS-7 cells. Western blot analysis was carried out on cell lysates prepared 48 h posttransfection (Fig. 1B). We found that although levels of UL24-I97A/I98A were lower than those of the other proteins, all the different versions of UL24 were expressed.

Differential impact of replacing conserved residues in UL24 on the dispersal of nucleolin. We next sought to test the impact of the mutations on the ability of UL24 to induce the dispersal of nucleolin. COS-7 cells were transiently transfected with each of the various HA-UL24 expression vectors. Forty-eight hours later, cells were fixed, permeabilized, and immunostained for HA (green) and nucleolin (red) (Fig. 2). Localization of HA-UL24 variants and of nucleolin was determined by confocal microscopy. We found that all substitution-containing forms of HA-UL24 exhibited strong perinuclear staining, which we have previously demonstrated corresponds to the Golgi apparatus, and speckled cytoplasmic staining, both similar to what has been seen for wild-type HA-UL24 (3). However, we observed a range of nuclear staining patterns for the different forms of HA-UL24. For the mutations H22L, Y26A, I97A/I98A, and E99A/K101A, protein localization in the nucleus was found predominantly in the nucleolus. In contrast, the staining pattern for L72A was similar to that seen for wild-type HA-UL24 in that there was diffuse nuclear staining in the vast majority of cells, with few cells exhibiting punctate nuclear staining. The pattern for E69A/V70A, R75A/D78A, Q117A, G121A, Q124A/L125A and Q154A was intermediate in that many cells showed the presence of weak nuclear foci of staining; however, the shape was distorted compared to the typical nucleolar staining pattern. We next quantitated the impact of the UL24 mutations on the distribution pattern seen for nucleolin in these cells. For each mutation, we counted the number of cells expressing HA-UL24 that retained nuclear foci of nucleolin staining. In each case, the status of nucleolin staining was determined for more than 100 transfected cells in three independent assays. Each result presented represents the average from the three experiments and the standard deviation (Fig. 3). We found that the localization of nucleolin also varied depending on the UL24 substitution analyzed. For wild-type UL24, only ≈16% of cells expressing HA-UL24 exhibited the characteristic punctate nucleolar staining for nucleolin, similar to what we have previously shown. For the mutations, three groups were observed. The substitutions H22L, Y26A, I97A/I98A, and E99A/K101A severely affected the ability of UL24 to modify nucleoli, such that the number of cells retaining clear foci of nucleolin staining was greater than 60%. The E69A/V70A, R75A/D78A, Q117A, G121A, Q124A/L125A, and Q154A mutations had only a slight to moderate effect, with between 20 and 45% of cells exhibiting the typical strong foci of nucleolin staining while the majority of cells showed only weak, distorted foci of staining or diffuse staining. Interestingly, the L72A mutation did not appear to have any effect on the ability of UL24 to induce the dispersal of nucleolin in that only 9% of cells retained foci of nucleolin staining. Thus, highly conserved residues in UL24 were of variable importance for the ability of this protein to modify nucleoli.

Construction and characterization of vUL24-eGFP. To allow for quick screening of recombinant viruses with mutations in *UL24*, we first constructed a virus where *UL24* was disrupted by insertion of the gene for eGFP driven by a CMV promoter (Fig. 4A). The resulting virus, vUL24-eGFP, produced eGFP but no longer had a functional *UL24* gene. Two independent isolates of vUL24-eGFP (b and c) were produced. To ensure that any phenotypes we ultimately observed in viruses engineered to contain *UL24* mutations were due to the inserted mutations and not to a

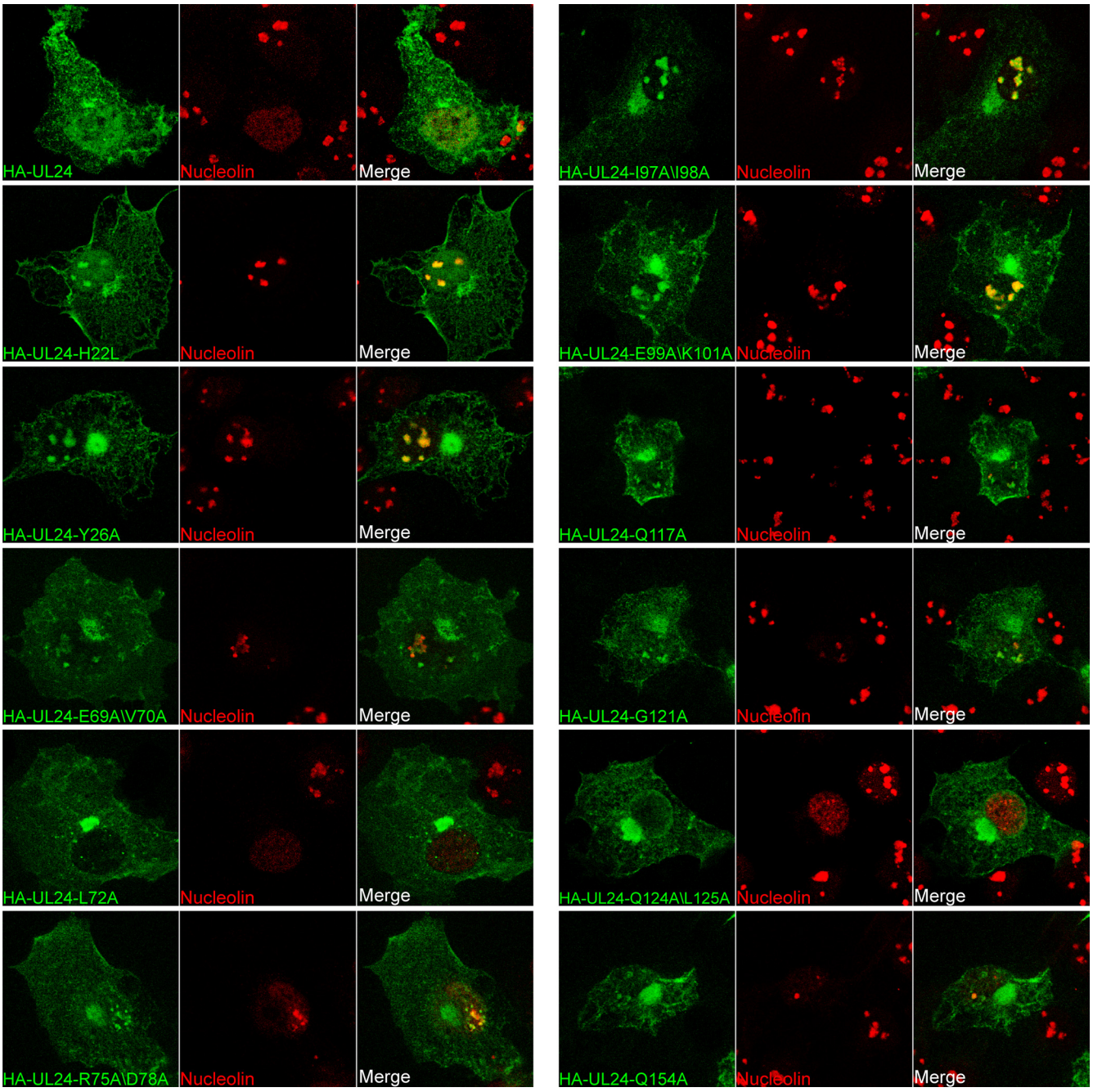

FIG. 2. Impact of UL24 variants on the localization of nucleolin. Confocal images of COS-7 cells transiently expressing different forms of HA-UL24 with the indicated amino acid substitutions or with the wild-type UL24 sequence and immunostained for HA-UL24 (green) and nucleolin (red). In each set of three panels, the left, middle, and right panels correspond to HA-UL24, nucleolin, and the merged image, respectively. Colocalization of the two signals is indicated by the yellow color in the merged panels.

change in the starting virus, we also constructed a rescue virus for vUL24-eGFPb. vUL24-eGFPbResc was generated by cotransfection of infectious DNA from vUL24-eGFPb with a transfer plasmid containing wild-type *UL24*. We characterized vUL24-eGFP prior to using it as the starting virus for the generation of the UL24 substitution mutants. The genome integrity of the viruses was confirmed by restriction digest and Southern blot analysis. Viral genomic DNA from KOS, vUL24-eGFPb and -c, vUL24-eGFPbResc, and the plasmids pAG5 and pBamHIQeGFP was digested with BamHI and resolved on an agarose gel (Fig. 4B). No difference in the overall digestion pattern was detected for the different viruses. The DNA was then transferred to a positively charged nylon membrane and analyzed by Southern blotting with a probe corresponding to pAG5, which contains the BamHI Q fragment in pBluescript II SK(+) (Fig. 4C). As expected, a band of approximately 3.5 kb was detected for each virus (see Fig. 4A), and an additional band

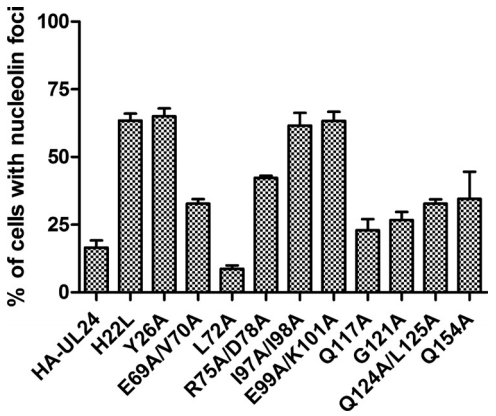

FIG. 3. Quantification of nucleolin distribution patterns in cells expressing HA-UL24 variants. COS-7 cells were transiently transfected with vectors expressing the HA-UL24 wild type or the substitution-containing forms indicated. Two days posttransfection, cells were costained for HA and nucleolin. The graph shows the percentage of cells expressing HA-UL24 that exhibited clear foci of nucleolin staining with little or no diffuse staining in the nucleus. Each result shown represents the average for three independent experiments, where more than 100 cells were analyzed for each mutation in each experiment. Error bars represent the standard errors of the means.

of 1.4 kb was seen for vUL24-eGFPb and -c. Thus, the overall genome organization for vUL24-eGFP was as expected.

A virus yield assay was carried out with the two vUL24-eGFP isolates and the rescue virus (Fig. 4D). We found that vUL24-eGFPb and -c replicated to titers half a $\log_{10}$ lower than those of the wild-type virus KOS. This is consistent with what has been shown previously for UL24-deficient viruses (18). In contrast, the rescue virus replicated to levels similar to those of KOS. To determine plaque phenotypes, Vero cells were infected at a low MOI, overlaid with medium containing methylcellulose, and incubated at 34, 37, or 39°C. Two days postinfection, images of the plaques were taken using a phase-contrast microscope (Fig. 4E). At 34°C, we did not detect a difference between the viruses. At 37°C, UL24X and vUL24-eGFPb and -c appeared to form somewhat smaller plaques than KOS or vUL24-eGFPResc. As expected, we found that both isolates of vUL24-eGFP (b and c) formed syncytial plaques at 39°C, similar to those observed with the UL24-null virus UL24X. In contrast, both the KOS virus and the rescue virus formed nonsyncytial plaques at 39°C. We concluded that our starting virus, vUL24-eGFPb, did not contain any mutations other than the eGFP insertion that impaired replication in cell culture or conferred a syncytial phenotype.

Construction and characterization of vUL24-E99A/K101A and vUL24-G121A. In order to assess whether the impact of the UL24 mutations in transfected cells reflected the impact in the context of infection, we selected two mutations, for which we constructed the corresponding mutant virus. We chose to introduce the mutation E99A/K101A, which targets the endonuclease motif and had a large impact on the ability of UL24 to disperse nucleolin, into the viral genome. We also chose a mutation, G121A, of another highly conserved residue that is not predicted to be part of this motif and which had only a moderate affect on nucleolin dispersal. Each of these residues is invariant among all the predicted UL24 proteins from the different herpesviruses sequenced to date. (There are currently 78 complete sequences of herpesvirus *UL24* homologs available in the NCBI database.) For consistency, all recombinant viruses were made using vUL24-eGFPb as a starting virus. Two independent isolates of each virus were produced. Expression of the modified forms of UL24 was confirmed by Western blot analysis of cell lysates harvested 18 hpi (Fig. 5A and B). The blot was probed for UL24 and then stripped and probed for ICP8 as an internal control. We noted that vUL24-E99A/K101A migrated slightly faster than wild-type UL24. We often detected a similar shift in lysates from transiently transfected cells. However, both UL24-E99A/K101A and UL24-G121A were expressed at levels similar to those of UL24 in KOS.

We carried out a viral yield assay on the UL24 mutant viruses. We found that the E99A/K101A mutation reduced viral titers by approximately half a $\log_{10}$ (Fig. 5C); however, the G121A mutation resulted in replication levels similar to those of KOS (Fig. 5C). We next tested whether the mutations affected the plaque phenotype (Fig. 5D and E). We found that both vUL24-E99A/K101A and vUL24-G121A, which have mutations in different HDs, resulted in the formation of syncytial plaques at 39°C, similar to those formed by UL24X. Thus, substitutions targeting highly conserved residues in different HDs conferred a syncytial plaque phenotype, while only the mutation affecting the endonuclease motif appeared to affect viral replication.

Substitution of highly conserved residues in UL24 causes defects in HSV-1-induced dispersal of nucleolin. To determine whether the effect of the UL24 substitutions on nucleolin in transfected cells reflected the importance of the residues during infection, we tested the impact of the mutations on the ability of HSV-1 to modify nucleoli. Vero cells were grown on coverslips and either mock infected or infected with vUL24-E99A/K101Aa and -b, vUL24-G121Aa and -b, KOS, or UL24X. Cells were fixed at 18 hpi and immunostained for nucleolin (green), and the nuclei were stained with Draq5 (blue) (Fig. 6A). As we have seen previously, we observed foci of nucleolin in very few KOS-infected cells (less than 2%), while the majority of cells infected with UL24X retained foci of nucleolin (73%). vUL24-E99A/K101A resembled UL24X in that the majority of infected cells showed foci of nucleolin staining (60%), and vUL24-G121A exhibited an intermediate phenotype in that we detected clear foci of nucleolin in only 28% of infected cells (Fig. 6B). Hence, we found that the effect of these mutations on the ability of UL24 to disperse nucleolin in the context of infection followed a trend similar to that observed in transfected cells. Our results are consistent with the notion that highly conserved residues in the endonuclease motif are particularly important for the ability of UL24 to induce the dispersal of nucleolin.

DISCUSSION

We previously demonstrated that UL24 is involved in the HSV-1-induced dispersal of nucleolin and that it plays an essential role in this process (3, 23). In this study, we furthered our investigation to identify residues important for this function and to test the hypothesis that the previously identified endonuclease motif was important for this activity.

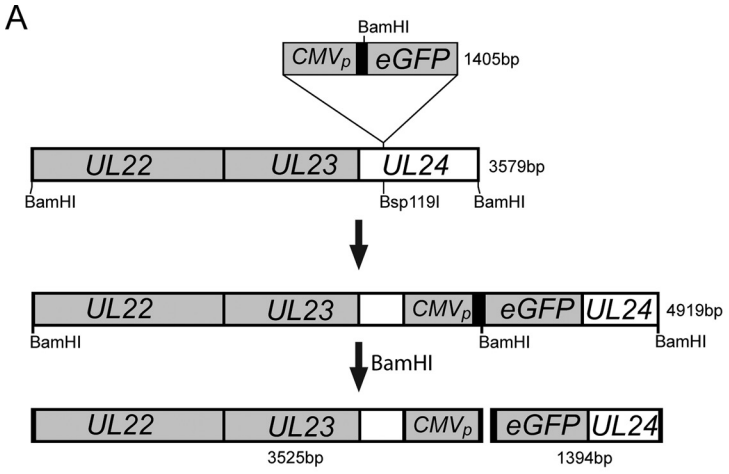
A
BamHI
CMVp
eGFP
1405bp
UL22
UL23
UL24
3579bp
BamHI
Bsp119I
BamHI
UL22
UL23
CMVp
eGFP
UL24
4919bp
BamHI
BamHI
BamHI
BamHI
UL22
UL23
CMVp
eGFP
UL24
3525bp
1394bp

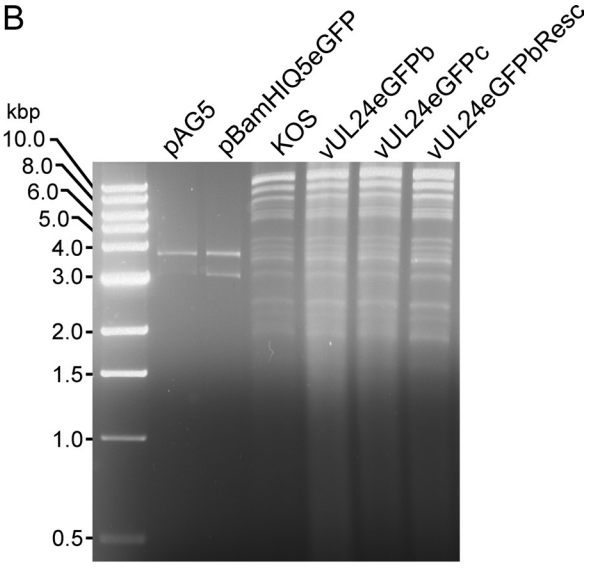
B
kbp
10.0
8.0
6.0
5.0
4.0
3.0
2.0
1.5
1.0
0.5
pAG5
pBamHIQ5eGFP
KOS
vUL24eGFPb
vUL24eGFPc
vUL24eGFPbResc

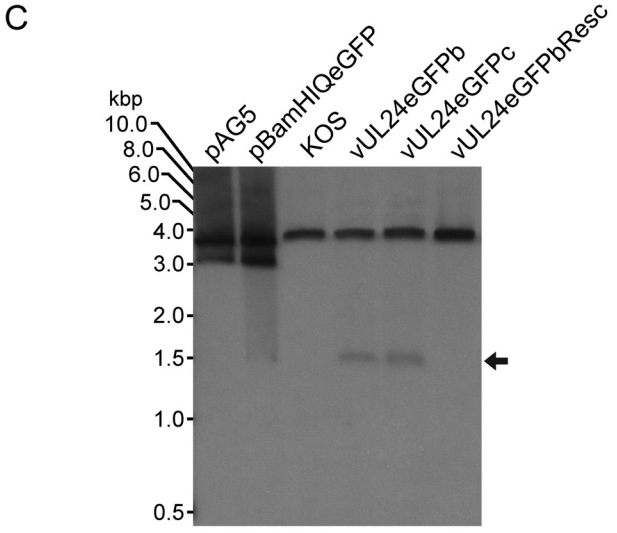
C
kbp
10.0
8.0
6.0
5.0
4.0
3.0
2.0
1.5
1.0
0.5
pAG5
pBamHIQeGFP
KOS
vUL24eGFPb
vUL24eGFPc
vUL24eGFPbResc

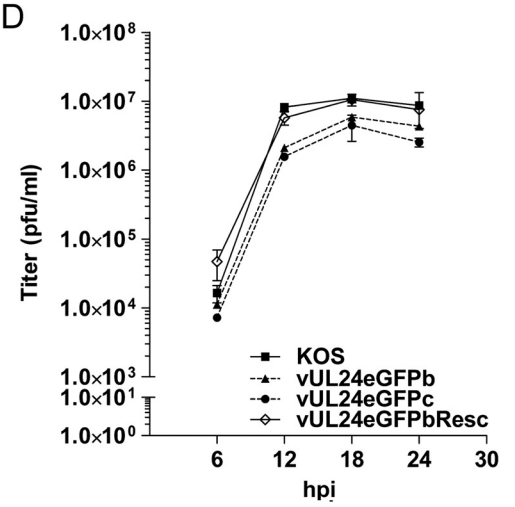
D
Titer (pfu/ml)
1.0×10^8
1.0×10^7
1.0×10^6
1.0×10^5
1.0×10^4
1.0×10^3
1.0×10^1
1.0×10^0
6
12
18
24
30
hpi
KOS
vUL24eGFPb
vUL24eGFPc
vUL24eGFPbResc

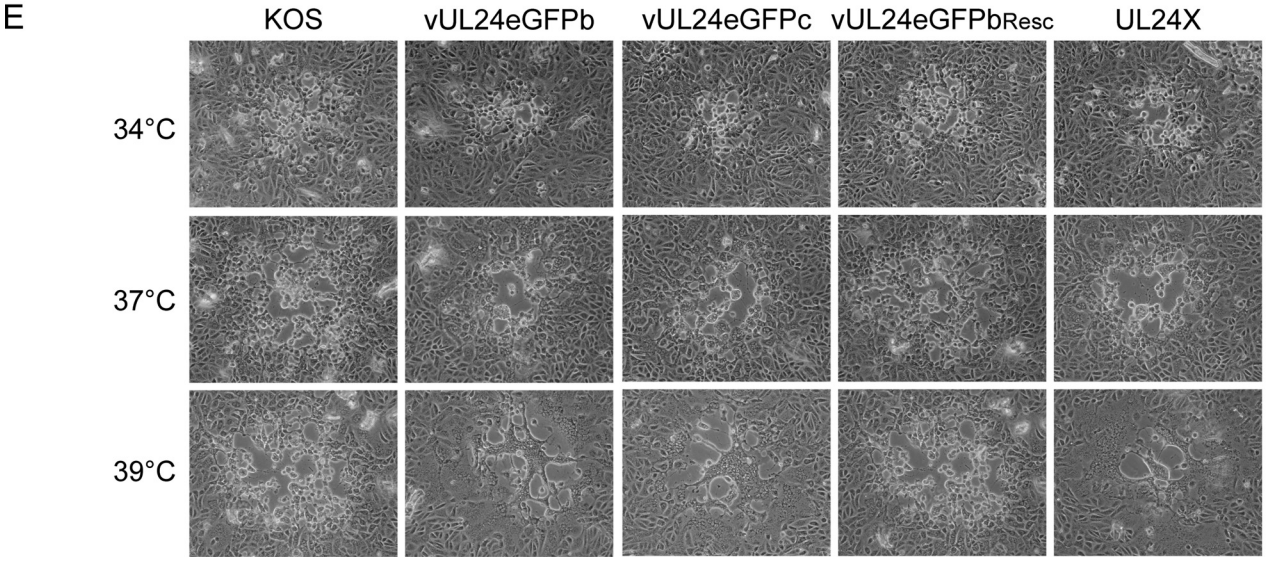
E
KOS
vUL24eGFPb
vUL24eGFPc
vUL24eGFPbResc
UL24X
34°C
37°C
39°C

Effect of replacing highly conserved residues on subcellular localization of UL24. In transiently transfected COS-7 cells, all of the modified HA-UL24 proteins retained perinuclear localization similar to that seen for the wild-type form of the protein (3). This result is consistent with our previous finding that the C-terminal portion of the protein alone localizes to the Golgi apparatus. The different nuclear staining patterns observed for the various substitution-containing forms of the protein correlated with that observed for nucleolin. Typically, in those cells where a particular HA-UL24 variant was present in clear nucleolar foci, nucleolin was also localized to nucleoli. In contrast, in cells where HA-UL24 was diffuse in the nucleus, we found that nucleolin staining was dispersed. Because we have previously shown that nucleolar localization is retained upon deletion of any one of the HDs, we conclude that the substitutions studied here did not affect the targeting of HA-UL24 to nucleoli. Rather, it is likely that all of the substitution forms tested localized to nucleoli but forms that retained the ability to alter nucleoli exhibited a concomitant change in the distribution pattern as this organelle was modified.

Importance of PD-(D/E)XK endonuclease motif for ability of UL24 to disperse nucleolin. Our results support the notion that the endonuclease motif is especially important for the effect of UL24 on nucleoli. Substitutions targeting the putative catalytic domain (E99A/K101A) or immediately adjacent to it (I97A/I98A), as well as residues that have been proposed to be important for substrate specificity (H22L and Y26A) (14, 20, 21), had the most dramatic effect. Although all substitution-containing forms of UL24 were expressed in COS-7 cells, we noted that UL24-I97A/I98A repeatedly exhibited reduced expression levels as determined by Western blot analysis on lysates from transiently transfected cells. Its expression, however, could easily be detected in our immunofluorescence assay and at an intensity apparently similar to that seen with the other modified versions of UL24. Regardless, we cannot exclude the possibility that the reduction in nucleolin dispersal seen for UL24-I97A/I98A was partially due to a reduced level of expression. Interestingly, several residues that were as well conserved as E99, K101, H22, and Y26, such as L72, Q117, and G121, did not appear to be of great importance for the ability of UL24 to disperse nucleolin.

Importance of highly conserved residues in UL24 during infection. The importance of the endonuclease motif for the dispersal of nucleolin also held true in the context of infection. Two independently derived isolates were obtained for each of the recombinant viruses vUL24-E99A/K101A and vUL24-G121A. We found that each pair of isolates behaved similarly. The E99A/K101A mutation caused a decrease in HSV-1-induced dispersal of nucleolin similar to that seen with the UL24-null virus. In contrast, the G121A mutation had only a moderate impact. These findings were consistent with our results in the transient transfection assays. Thus, the E99A/K101A mutation affects a site in the protein that is important for the effect of UL24 on nucleoli during infection. Furthermore, this mutation also caused a decrease in viral titers, suggesting that it affected a function important for efficient replication. UL12 is another HSV-1 protein with a nuclease motif and for which nuclease activity has been confirmed. UL12 may play a role in resolving X and Y DNA structures arising during viral DNA replication and in encapsidation (32). Nuclease activity has not yet been reported for UL24; however, the discovery that the motif is important for the function of the protein suggests that UL24 may indeed possess a nuclease function. Evidence is accumulating that the nucleolus is an organelle often targeted by viruses to increase their replication efficiency and circumvent cellular control systems (12, 17). Adenovirus induces the redistribution of the nucleolar proteins nucleolin and B23 to the cytoplasm (25), and poliovirus also causes the relocalization of nucleolin to the cytoplasm (41). The nucleolus is involved in cell cycle regulation, and the coronavirus N protein binds nucleolin and disrupts cytokenesis (8, 43). A role for nucleolar localization and viral mRNA transport to the cytoplasm has been shown for the human immunodeficiency virus protein Rev (28) and herpesvirus samiri ORF57 (6). Further experiments will be required to establish the mechanism underlying the effect of UL24 on nucleoli and the function of this cellular modification in infection.

Replacement of highly conserved residues in UL24 causes syncytial plaques. vUL24-E99A/K101A was impaired for viral replication in cell culture, while vUL24-G121A replicated to titers similar to those seen for KOS. However, both the E99A/K101A and G121A mutations caused a syncytial plaque phenotype at 39°C. Therefore, even though the G121A change is a conservative substitution, it did have an impact on at least one function of the protein during infection. Thus, the E99A/K101A mutation resulted in a phenotype resembling that of a UL24-null virus, while the G121A mutation appeared to affect only the formation of syncytia. In transient transfection assays, both UL24-E99A/K101A and UL24-G121A localized to the Golgi apparatus in a manner similar to that seen for the wild-type protein. This perinuclear localization was consistent with

FIG. 4. vUL24-eGFP. (A) Schematic representation of the insertion of an eGFP expression cassette in the *UL24* ORF and the resulting BamHI fragments. The gray boxes represent the genes present in the BamHI Q fragment of the HSV-1 genome and the inserted eGFP expression cassette. The *UL24* ORF is denoted by a white box. The black box between the CMV promoter and the eGFP gene represents the multiple cloning site from the plasmid pEGFP-N1. The top section represents the wild-type BamHI Q fragment and the insertion site of the eGFP cassette. The middle section represents the BamHI Q fragment following insertion. The bottom section shows the fragments obtained after BamHI digestion. (B) Genome analysis of vUL24-eGFPb and -c and vUL24-eGFPbResc. The ethidium bromide-stained agarose gel shows fragments generated following BamHI digestion of viral DNA and control plasmids. Plasmids contained either the wild-type BamHI Q fragment (pAG5) or the fragment containing the eGFP insertion (pBamH1QeGFP). Positions of the molecular mass markers are indicated to the left of the panel. (C) Southern blot analysis using a probe corresponding to the BamHI Q fragment in pBluescript II SK(+). The arrow to the right of the panel indicates the position of the fragment generated due to the insertion of the eGFP cassette. (D) Characterization of vUL24-eGFP viruses and vUL24-eGFPResc in a one-step growth curve. Results shown represent the average for two independent experiments done in duplicate. Error bars represent the standard errors of the means. (E) Plaque morphology was assessed for the different viruses on Vero cells 2 days postinfection grown at the indicated temperatures.

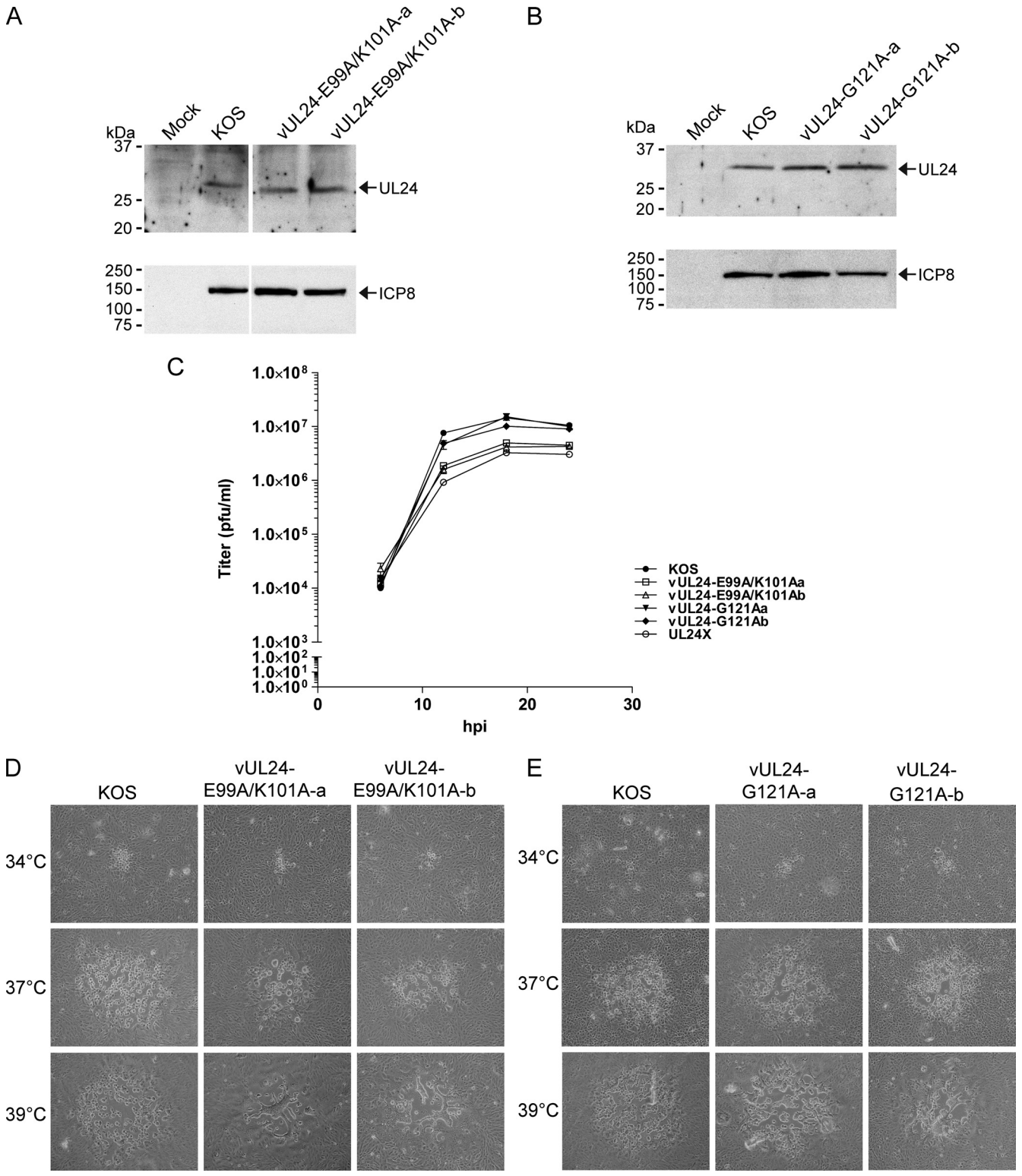

FIG. 5. Characterization of vUL24-E99A/K101A and vUL24-G121A. (A) Western blot showing expression of UL24 in Vero cells infected with vUL24-E99A/K101A (a and b) (top panel). The blot was stripped and reblotted for the viral protein ICP8 as a control (bottom panel). (B) Western blot showing expression of UL24 in cells infected with vUL24-G121Aa and -b (top panel). The blot was stripped and reblotted for the viral protein ICP8 as a control (bottom panel). The positions of molecular mass markers are indicated to the left of each panel. Arrows to the right of the panels mark the position of the protein. (C) One-step growth analysis of vUL24-E99A/K101A (isolates a and b) and vUL24-G121A (isolates a and b) compared to the wild-type virus KOS and the UL24-deficient virus UL24X. (D) Analysis of plaque morphology for vUL24-E99A/K101Aa and -b or (E) for vUL24-G121Aa and -b on Vero cells at 2 days postinfection grown at the indicated temperatures.

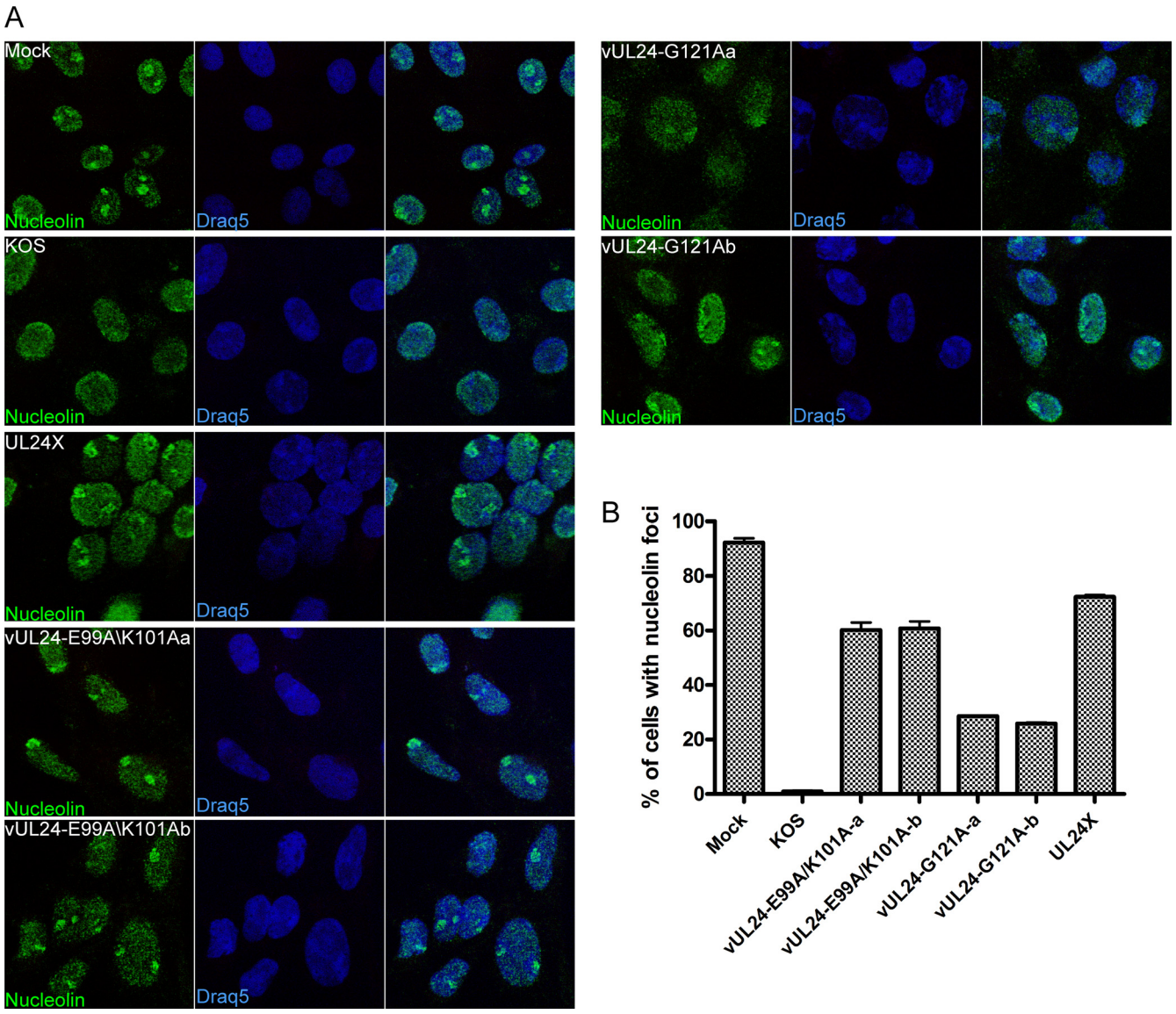

FIG. 6. Distribution pattern of nucleolin in Vero cells infected with UL24 mutants. (A) Confocal images of cells either mock infected or infected with the indicated virus. Cells were immunostained for nucleolin (green), and nuclei were stained with Draq5 (blue). Left-hand panels show nucleolin localization, center panels show stained nuclei, and merged images are shown in the right-hand panels. (B) Quantification of the distribution pattern for nucleolin in cells infected with the indicated UL24 mutants. Cells were either mock infected or infected at an MOI of 10 and stained for nucleolin at 18 hpi. Cells were analyzed by confocal microscopy, and the number of cells showing clear foci of nucleolin staining was scored. Each result shown represents the average for two independent experiments in which the localization of nucleolin in more than 150 cells was analyzed for each mutant virus. Error bars represent the standard errors of the means.

our previous observation that the C-terminal portion of UL24 is sufficient to target the Golgi apparatus (3). However, this result also suggests that the conserved N-terminal region of UL24 is dispensable for Golgi localization yet is important for the ability of UL24 to inhibit aberrant cell fusion during infection. Furthermore, because vUL24-G121A replicated to titers similar to those of wild-type virus, this also suggests that the *UL24*-associated syncytial phenotype is not inextricably associated with a reduction in HSV-1 replication in cell culture.

The results from this mutagenesis study support the hypothesis that UL24 has at least two distinct functions during infection: namely, a role in HSV-1-induced nucleolar modifications and a role in modulating membrane fusion. The UL24 protein is detected both in the nucleus and in the cytoplasm of cells (3, 23, 31). In our model, UL24 transiently localizes to nucleoli and participates in the remodelling of this organelle during infection. We have shown that this function depends on the endonuclease motif, and we propose that it contributes to the efficiency of a nuclear event in the viral life cycle, possibly by releasing cellular factors involved in viral DNA replication or gene expression. This would explain why a mutation targeting the endonuclease motif resulted in a decrease in viral yield. A second role for UL24 would be in the cytoplasm, where the protein localizes to Golgi-related vesicles and affects mem-

brane fusion events related to virion morphogenesis. In the absence of UL24, we propose that the function of viral or cellular proteins involved in fusion is altered, leading to aberrant fusion events and the formation of syncytia while not inhibiting the formation of new infectious viral particles.

In summary, our mutational analysis has established the importance of the endonuclease motif in UL24 for the dispersal of nucleolin. Although our results are consistent with a link between UL24-dependent dispersal of nucleolin and the efficiency of viral replication, further studies will be required to establish such a correlation and to determine whether UL24 possesses an endonuclease activity.

ACKNOWLEDGMENTS

L.B. was supported by graduate scholarships from the Canadian Institutes for Health Research (CIHR), the Fonds pour la Recherche en Santé du Québec (FRSQ), and Fondation Armand-Frappier. G.A.L.-T. was supported by a graduate scholarship from FRSQ. This project was funded through an infrastructure grant from the Canada Foundation for Innovation and an operating grant from CIHR to A.P.

We thank D. M. Coen (Harvard Medical School) for the viral strains KOS and UL24X and A. Griffiths for comments on the manuscript.

REFERENCES

1. **Avitabile, E., G. Lombardi, T. Gianni, M. Capri, and G. Campadelli-Fiume.** 2004. Coexpression of UL20p and gK inhibits cell-cell fusion mediated by herpes simplex virus glycoproteins gD, gH-gL, and wild-type gB or an endocytosis-defective gB mutant and downmodulates their cell surface expression. J. Virol. **78:**8015–8025.
2. **Baines, J. D., P. L. Ward, G. Campadelli-Fiume, and B. Roizman.** 1991. The UL20 gene of herpes simplex virus 1 encodes a function necessary for viral egress. J. Virol. **65:**6414–6424.
3. **Bertrand, L., and A. Pearson.** 2008. The conserved N-terminal domain of herpes simplex virus 1 UL24 protein is sufficient to induce the spatial redistribution of nucleolin. J. Gen. Virol. **89:**1142–1151.
4. **Besse, S., and F. Puvion-Dutilleul.** 1996. Distribution of ribosomal genes in nucleoli of herpes simplex virus type 1 infected cells. Eur. J. Cell Biol. **71:**33–44.
5. **Boisvert, F. M., S. van Koningsbruggen, J. Navascues, and A. I. Lamond.** 2007. The multifunctional nucleolus. Nat. Rev. Mol. Cell Biol. **8:**574–585.
6. **Boyne, J. R., and A. Whitehouse.** 2006. Nucleolar trafficking is essential for nuclear export of intronless herpesvirus mRNA. Proc. Natl. Acad. Sci. U. S. A. **103:**15190–15195.
7. **Bzik, D. J., B. A. Fox, N. A. DeLuca, and S. Person.** 1984. Nucleotide sequence of a region of the herpes simplex virus type 1 gB glycoprotein gene: mutations affecting rate of virus entry and cell fusion. Virology **137:**185–190.
8. **Chen, H., T. Wurm, P. Britton, G. Brooks, and J. A. Hiscox.** 2002. Interaction of the coronavirus nucleoprotein with nucleolar antigens and the host cell. J. Virol. **76:**5233–5250.
9. **Davison, A. J.** 1992. Channel catfish virus: a new type of herpesvirus. Virology **186:**9–14.
10. **Davison, A. J.** 2002. Evolution of the herpesviruses. Vet. Microbiol. **86:**69–88.
11. **Diakidi-Kosta, A., G. Michailidou, G. Kontogounis, A. Sivropoulou, and M. Arsenakis.** 2003. A single amino acid substitution in the cytoplasmic tail of the glycoprotein B of herpes simplex virus 1 affects both syncytium formation and binding to intracellular heparan sulfate. Virus Res. **93:**99–108.
12. **Emmott, E., and J. A. Hiscox.** 2009. Nucleolar targeting: the hub of the matter. EMBO Rep. **10:**231–238.
13. **Engel, J. P., E. P. Boyer, and J. L. Goodman.** 1993. Two novel single amino acid syncytial mutations in the carboxy terminus of glycoprotein B of herpes simplex virus type 1 confer a unique pathogenic phenotype. Virology **192:** 112–120.
14. **Feder, M., and J. M. Bujnicki.** 2005. Identification of a new family of putative PD-(D/E)XK nucleases with unusual phylogenomic distribution and a new type of the active site. BMC Genomics **6:**21.
15. **Goodman, J. L., and J. P. Engel.** 1991. Altered pathogenesis in herpes simplex virus type 1 infection due to a syncytial mutation mapping to the carboxy terminus of glycoprotein B. J. Virol. **65:**1770–1778.
16. **Griffiths, A., and D. M. Coen.** 2003. High-frequency phenotypic reversion and pathogenicity of an acyclovir-resistant herpes simplex virus mutant. J. Virol. **77:**2282–2286.
17. **Hiscox, J. A.** 2002. The nucleolus—a gateway to viral infection? Arch. Virol. **147:**1077–1089.
18. **Jacobson, J. G., S. H. Chen, W. J. Cook, M. F. Kramer, and D. M. Coen.** 1998. Importance of the herpes simplex virus UL24 gene for productive ganglionic infection in mice. Virology **242:**161–169.
19. **Jacobson, J. G., S. L. Martin, and D. M. Coen.** 1989. A conserved open reading frame that overlaps the herpes simplex virus thymidine kinase gene is important for viral growth in cell culture. J. Virol. **63:**1839–1843.
20. **Knizewski, L., L. Kinch, N. V. Grishin, L. Rychlewski, and K. Ginalski.** 2006. Human herpesvirus 1 UL24 gene encodes a potential PD-(D/E)XK endonuclease. J. Virol. **80:**2575–2577.
21. **Kosinski, J., M. Feder, and J. M. Bujnicki.** 2005. The PD-(D/E)XK superfamily revisited: identification of new members among proteins involved in DNA metabolism and functional predictions for domains of (hitherto) unknown function. BMC Bioinformatics **6:**172.
22. **Lopez, M. R., E. F. Schlegel, S. Winterstteller, and J. A. Blaho.** 2008. The major tegument structural protein VP22 targets areas of dispersed nucleolin and marginalized chromatin during productive herpes simplex virus 1 infection. Virus Res. **136:**175–188.
23. **Lymberopoulos, M. H., and A. Pearson.** 2007. Involvement of UL24 in herpes-simplex-virus-1-induced dispersal of nucleolin. Virology **363:**397–409.
24. **MacLean, C. A., F. J. Rixon, and H. S. Marsden.** 1987. The products of gene US11 of herpes simplex virus type 1 are DNA-binding and localize to the nucleoli of infected cells. J. Gen. Virol. **68**(Pt. 7)**:**1921–1937.
25. **Matthews, D. A.** 2001. Adenovirus protein V induces redistribution of nucleolin and B23 from nucleolus to cytoplasm. J. Virol. **75:**1031–1038.
26. **Maul, G. G., H. H. Guldner, and J. G. Spivack.** 1993. Modification of discrete nuclear domains induced by herpes simplex virus type 1 immediate early gene 1 product (ICP0). J. Gen. Virol. **74**(Pt. 12)**:**2679–2690.
27. **Maul, G. G., A. M. Ishov, and R. D. Everett.** 1996. Nuclear domain 10 as preexisting potential replication start sites of herpes simplex virus type-1. Virology **217:**67–75.
28. **Meyer, B. E., and M. H. Malim.** 1994. The HIV-1 Rev trans-activator shuttles between the nucleus and the cytoplasm. Genes Dev. **8:**1538–1547.
29. **Monier, K., J. C. Armas, S. Etteldorf, P. Ghazal, and K. F. Sullivan.** 2000. Annexation of the interchromosomal space during viral infection. Nat. Cell Biol. **2:**661–665.
30. **Morency, E., Y. Coute, J. Thomas, P. Texier, and P. Lomonte.** 2005. The protein ICP0 of herpes simplex virus type 1 is targeted to nucleoli of infected cells. Brief report. Arch. Virol. **150:**2387–2395.
31. **Pearson, A., and D. M. Coen.** 2002. Identification, localization, and regulation of expression of the UL24 protein of herpes simplex virus type 1. J. Virol. **76:**10821–10828.
32. **Porter, I. M., and N. D. Stow.** 2004. Replication, recombination and packaging of amplicon DNA in cells infected with the herpes simplex virus type 1 alkaline nuclease null mutant ambUL12. J. Gen. Virol. **85:**3501–3510.
33. **Reynolds, A. E., L. Liang, and J. D. Baines.** 2004. Conformational changes in the nuclear lamina induced by herpes simplex virus type 1 require genes U(L)31 and U(L)34. J. Virol. **78:**5564–5575.
34. **Ruyechan, W. T., L. S. Morse, D. M. Knipe, and B. Roizman.** 1979. Molecular genetics of herpes simplex virus. II. Mapping of the major viral glycoproteins and of the genetic loci specifying the social behavior of infected cells. J. Virol. **29:**677–697.
35. **Salsman, J., N. Zimmerman, T. Chen, M. Domagala, and L. Frappier.** 2008. Genome-wide screen of three herpesviruses for protein subcellular localization and alteration of PML nuclear bodies. PLoS Pathog. **4:**e1000100.
36. **Sanders, P. G., N. M. Wilkie, and A. J. Davison.** 1982. Thymidine kinase deletion mutants of herpes simplex virus type 1. J. Gen. Virol. **63:**277–295.
37. **Scott, E. S., and P. O'Hare.** 2001. Fate of the inner nuclear membrane protein lamin B receptor and nuclear lamins in herpes simplex virus type 1 infection. J. Virol. **75:**8818–8830.
38. **Silverstein, S., and D. L. Engelhardt.** 1979. Alterations in the protein synthetic apparatus of cells infected with herpes simplex virus. Virology **95:**334–342.
39. **Tognon, M., R. Guandalini, M. G. Romanelli, R. Manservigi, and B. Trevisani.** 1991. Phenotypic and genotypic characterization of locus Syn 5 in herpes simplex virus 1. Virus Res. **18:**135–150.
40. **Uprichard, S. L., and D. M. Knipe.** 1997. Assembly of herpes simplex virus replication proteins at two distinct intranuclear sites. Virology **229:**113–125.
41. **Waggoner, S., and P. Sarnow.** 1998. Viral ribonucleoprotein complex formation and nucleolar-cytoplasmic relocalization of nucleolin in poliovirus-infected cells. J. Virol. **72:**6699–6709.
42. **Wagner, E. K., and B. Roizman.** 1969. Ribonucleic acid synthesis in cells infected with herpes simplex virus. I. Patterns of ribonucleic acid synthesis in productively infected cells. J. Virol. **4:**36–46.
43. **Wurm, T., H. Chen, T. Hodgson, P. Britton, G. Brooks, and J. A. Hiscox.** 2001. Localization to the nucleolus is a common feature of coronavirus nucleoproteins, and the protein may disrupt host cell division. J. Virol. **75:**9345–9356.